

Ab initio simulation of single vibronic level fluorescence spectra of anthracene using Hagedorn wavepackets

Zhan Tong Zhang and Jiří J. L. Vaníček*

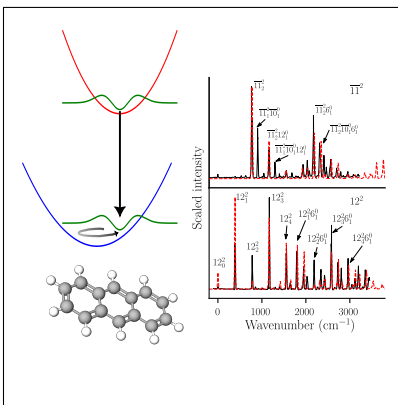
*Laboratory of Theoretical Physical Chemistry, Institut des Sciences et Ingénierie Chimiques,
Ecole Polytechnique Fédérale de Lausanne (EPFL), CH-1015 Lausanne, Switzerland*

E-mail: jiri.vanicek@epfl.ch

Abstract

Single vibronic level (SVL) fluorescence spectroscopy contributes to the understanding of molecular vibrational structures and relaxation processes. Here, we present a practical method for computing SVL fluorescence spectra of polyatomic molecules from arbitrary initial vibrational levels. This method, which combines a time-dependent approach using Hagedorn wavepackets with accurate evaluation of electronic structure, captures both mode distortion and Duschinsky rotation. We apply the method to compute SVL spectra of anthracene by performing wavepacket dynamics on a 66-dimensional harmonic potential energy surface constructed from density functional theory calculations. With the Hagedorn approach, we not only reproduce the previously reported simulation results for singly excited 12^1 and $\overline{11}^1$ levels, but also are able to compute SVL spectra from multiply excited levels in good agreement with experiments. All spectra were obtained from the same wavepacket trajectory without any additional propagation beyond what is required for ground-state emission spectra.

TOC Graphic



Single vibronic level (SVL) fluorescence spectroscopy measures the fluorescence decay of a system following a vibronic excitation to a specific vibrational level in the excited electronic state. This spectroscopic tool has played an important role in investigations of excited-state relaxation pathways,^{1,2} intramolecular vibrational energy redistribution processes,³⁻⁶ vibrational structures of ground and excited electronic states,^{4,7,8} as well as in the identification and characterization of rotamers and reactive intermediates.⁹⁻¹² To better understand these spectra and guide experiments, computational methods based on ab initio electronic structure calculations have been developed and implemented.¹³⁻¹⁹

Calculations of SVL spectra have mostly relied on the time-independent approach where individual Franck-Condon factors are computed for each vibronic transition.^{13,14,19,20} However, for larger polyatomic molecules, the task becomes challenging due to the large number of possible transitions and the computation of nonseparable overlap integrals, especially in the presence of Duschinsky mixing effects and when anharmonicity corrections to the vibrational wavefunctions and energy levels are necessary.²¹⁻²⁴ The time-dependent approach, which is more fundamental, avoids the need to prescreen transitions and can more naturally accommodate Duschinsky rotation,^{17,25,26} anharmonicity,²⁷⁻³⁰ Herzberg-Teller,^{25,28,29,31-36} and temperature effects³⁷⁻⁴⁰ in both linear and multidimensional⁴¹⁻⁴⁴ vibronic spectra.

Tapavicza combined the time-dependent approach to SVL spectra with a generating-function-based method to simulate emissions from a singly excited state (i.e., at most an excitation to the first excited vibrational level in one mode only).¹⁷ Using a displaced, distorted, and Duschinsky-rotated global harmonic model, he successfully computed SVL spectra of singly excited anthracene in very good agreement with the experimental results.⁴

In order to evaluate SVL emission from arbitrary vibronic levels, we recently proposed⁴⁵ another time-dependent approach based on Hagedorn wavepackets.⁴⁶⁻⁴⁸ These wavepackets in the form of a Gaussian multiplied by a carefully constructed polynomial⁴⁸⁻⁵⁰ are exact solutions of the time-dependent Schrödinger equation with a quadratic potential and have attracted interest in applied mathematics^{47-49,51-57} for their applications in physics and

chemistry.^{58–62} With the recursive expressions we derived for their overlap integrals,⁶³ the application of Hagedorn wavepackets in spectroscopy is now possible. In ref 45, we validated the Hagedorn dynamics approach to compute SVL spectra against quantum split-operator results in two-dimensional harmonic model systems incorporating displacement, mode distortion, and Duschinsky rotation effects.

To extend the approach from ref 45 to realistic, polyatomic molecules, here we neglect ro-vibrational coupling and perform the vibrational Hagedorn wavepacket dynamics on a full-dimensional, global harmonic potential energy surface derived from accurate electronic structure calculations. As a test, we simulate the SVL spectra of anthracene from $\overline{11}^j$ and 12^j ($j = 1, 2$) levels, for which assigned experimental data are available.⁴ We also predict the SVL spectra from the 6^112^1 , $\overline{5}^112^1$, and 5^112^1 levels, which remain to be measured experimentally. Whereas the singly excited cases were already successfully simulated by Tapavizca,¹⁷ our Hagedorn approach can also treat higher and mixed excitations at a negligible additional cost.

In the time-dependent approach to vibronic spectroscopy, the spectrum is evaluated as the Fourier transform of an appropriate wavepacket autocorrelation function

$$C(t) = \langle \psi_0 | \psi_t \rangle, \quad (1)$$

i.e., the overlap between the initial nuclear wavepacket ψ_0 and the wavepacket ψ_t propagated to time t on the final electronic surface. In the case of SVL fluorescence spectrum, the emission rate per unit frequency from a vibrational level $\psi_0 = |K\rangle$ on the excited electronic surface e is given by

$$\sigma_{\text{em}}(\omega) = \frac{4\omega^3}{3\pi\hbar c^3} |\mu_{ge}|^2 \text{Re} \int_0^\infty \overline{C(t)} \exp[it(\omega - \hbar\omega_{e,K})/\hbar] dt, \quad (2)$$

where $K \equiv (K_1, \dots, K_D)$ is a multi-index specifying the initial vibrational quantum numbers in the D normal modes, μ_{ge} is the electronic transition dipole moment (within the Condon

approximation), \hat{H}_g is the electronic ground state Hamiltonian, and $\hbar\omega_{e,K}$ is the vibrational energy of the initial state.

For the conventional emission spectrum from the ground level $K = \mathbf{0}$, the initial state may be represented by a normalized D -dimensional Gaussian wavepacket

$$\varphi_0(q) = \frac{1}{(\pi\hbar)^{D/4} \sqrt{\det(Q_t)}} \exp \left\{ \frac{i}{\hbar} \left[\frac{1}{2} x^T \cdot P_t \cdot Q_t^{-1} \cdot x + p_t^T \cdot x + S_t \right] \right\} \quad (3)$$

in Hagedorn's parametrization, where $x := q - q_t$ is the shifted position, q_t and p_t are the position and momentum of the center of the wavepacket, S_t is the classical action, and Q_t and P_t are complex-valued D -dimensional matrices replacing the more common width matrix $A_t \equiv P_t \cdot Q_t^{-1}$ in Heller's parametrization^{64,65} and satisfying the symplecticity conditions^{48,55}

$$Q_t^T \cdot P_t - P_t^T \cdot Q_t = 0, \quad (4)$$

$$Q_t^\dagger \cdot P_t - P_t^\dagger \cdot Q_t = 2i\text{Id}_D. \quad (5)$$

We can then apply the Hagedorn raising operator

$$A^\dagger := \frac{i}{\sqrt{2\hbar}} \left(P_t^\dagger \cdot (\hat{q} - q_t) - Q_t^\dagger \cdot (\hat{p} - p_t) \right) \quad (6)$$

to the Gaussian wavepacket φ_0 to generate an orthonormal family of Hagedorn functions

$$\varphi_{K+\langle j \rangle} = \frac{1}{\sqrt{K_j + 1}} A_j^\dagger \varphi_K \quad (7)$$

in the form of multivariate polynomials multiplying a common Gaussian, where $\langle j \rangle = (0, \dots, 0, 1, 0, \dots, 0)$ is the j -th unit vector in D dimensions.^{46,48,55,66} When the matrix $Q_0^{-1} \overline{Q_0}$ is diagonal, the multidimensional Hagedorn function is a direct product of one-dimensional functions, each being a Gaussian multiplied by a Hermite polynomial. In the excited-state normal-mode coordinates, Hagedorn functions can therefore exactly represent the initial

state for SVL emission from any vibrational level $|K\rangle$ such that $\psi_0 = \varphi_K$.

Remarkably, Hagedorn wavepackets are exact solutions to the time-dependent Schrödinger equation with a harmonic potential

$$V(q) = v_0 + (q - q_{\text{ref}})^T \cdot \kappa \cdot (q - q_{\text{ref}})/2, \quad (8)$$

where the reference position q_{ref} , the reference energy v_0 , and the Hessian matrix κ may be determined from the results of ab initio electronic structure calculations. The time evolution of a Hagedorn wavepacket then follows particularly simple, classical-like equations

$$\begin{aligned} \dot{q}_t &= m^{-1} \cdot p_t, & \dot{p}_t &= -V'(q_t) \\ \dot{Q}_t &= m^{-1} \cdot P_t, & \dot{P}_t &= -\kappa \cdot Q_t, \\ \dot{S}_t &= L_t, & & \end{aligned} \quad (9)$$

with m being the mass matrix and L_t the Lagrangian.^{48,55,65} These equations of motion are the same as in the thawed Gaussian approximation, which has been applied to vibronic spectra arising from ground vibrational levels^{26,27,67,68} and can be extended to include a linear polynomial prefactor.^{33,35,38,69,70} Using Hagedorn wavepackets, it is possible to treat arbitrary polynomials times a Gaussian, and since the propagation (9) depends only on the Gaussian's parameters, a single Gaussian trajectory is sufficient to obtain SVL spectra from all vibrational levels. Importantly, if the Hessian matrix κ is not diagonal, the initially diagonal $Q_{t=0}$ matrix of the SVL initial state will no longer be diagonal under Duschinsky rotation, and the Hagedorn function will not be a simple direct product of univariate Hermite polynomials.^{48–50}

Figure 1 compares the SVL spectra of anthracene evaluated with the Hagedorn approach to the experimental spectra.⁴ Each simulated spectrum is shifted so that the transition to the ground vibrational level on the ground surface is at 0 cm^{-1} . To facilitate the comparison, the intensities of the highest peaks in all spectra (simulated and experimental) are set to one. In

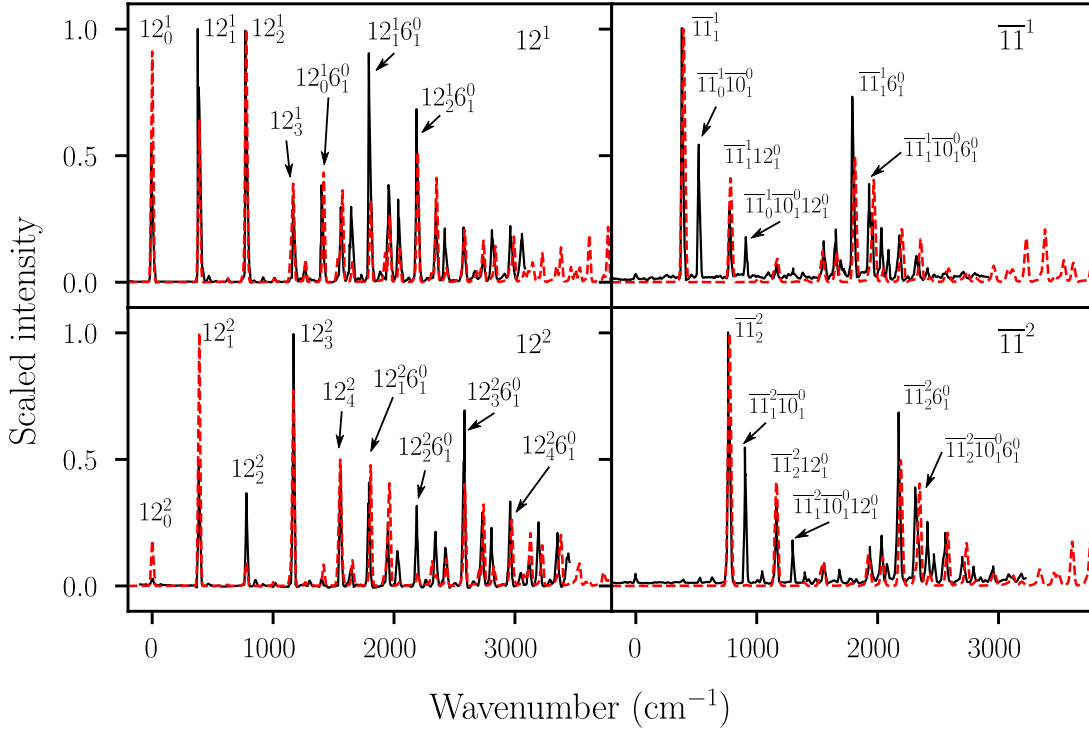


Figure 1: Comparison between the experimental (solid line) and simulated (dashed line) SVL fluorescence spectra of anthracene from initial vibrational levels 12^j and $\bar{11}^j$ ($j = 1, 2$); a scaling factor of 0.97 is applied to the wavenumbers.

addition, an empirical scaling factor is applied to the wavenumbers of the simulated spectra. By optimizing the alignment of peak positions between the simulated and experimental spectra, we set the scaling factor to 0.97, which is close to the vibrational scaling factors reported for the PBE0 functional with similar basis sets.⁷¹

The simulated spectra from singly excited levels agree surprisingly well with the experiment and are consistent with the results obtained by Tapavicza using a generating function approach.¹⁷ There, the underestimation of $\bar{11}_0^1 \bar{10}_1^0$ and $\bar{11}_0^1 \bar{10}_1^0 12_1^0$ peaks in the $\bar{11}^1$ spectrum was attributed to the underestimation of Duschinsky coupling between modes $\bar{11}$ and $\bar{10}$ by the electronic structure programs for both second-order approximate coupled cluster (CC2) and density functional theory (DFT) methods.

In contrast to ref 17, the Hagedorn approach makes it possible to compute SVL spectra

from multiply excited levels. Figure 1 compares our Hagedorn results to the experimental spectra for levels 12^2 and $\overline{11}^2$. While both simulated spectra agree rather well with the experiments, we observe a few missing or significantly underestimated peaks ($\overline{11}_1^2\overline{10}_1^0$, $\overline{11}_1^2\overline{10}_1^0 12_1^0$, and $\overline{11}_1^2\overline{10}_1^0 12_2^0$) in the simulated SVL spectrum from the $\overline{11}^2$ level. As explained and demonstrated in ref 45, the Hagedorn wavepacket approach is exact in global harmonic potentials. Therefore, the differences between experimental and simulated spectra here must be due to the inaccuracies of the global harmonic model from electronic structure calculations (e.g., underestimation of Duschinsky effects), significant anharmonicity of the true potential energy surface, or possibly experimental error.

Other than the shift of $\overline{11}_j^j$ transitions, the SVL spectra from $\overline{11}^1$ and $\overline{11}^2$ levels are broadly similar in structure experimentally. The similar structures of the spectra from the two levels are also evident in the simulated spectra. However, significant differences in intensity patterns exist between the 12^1 and 12^2 spectra. The computed 12^2 spectrum captures correctly the decrease in intensity observed experimentally for the 12_0^j , 12_j^j , and $12_j^j 6_1^0$ peaks.

If we do not apply empirical wavenumber scaling, the discrepancies in frequencies between the simulated and experimental spectra become obvious at higher wavenumbers (Fig. 2). For anthracene, the empirical scaling primarily compensates for the anharmonicity of the true potential energy surface. To effectively capture anharmonic effects and potentially eliminate the need for an arbitrary scaling factor, the time-dependent Hagedorn approach may further employ the local harmonic approximation with an on-the-fly trajectory of ab initio calculations. This may be particularly important for smaller, less rigid molecules, which will be the subject of our further studies.

Our method can treat not only multiple excitations in a single mode, but also initial states where several vibrational modes are simultaneously excited to any vibrational level. Figure 3 shows the predicted SVL emission spectra from the levels $6^1 12^1$, $\overline{5}^1 12^1$, and $5^1 12^1$. These simulated spectra present some similar features as the simulated 12^1 spectrum, but

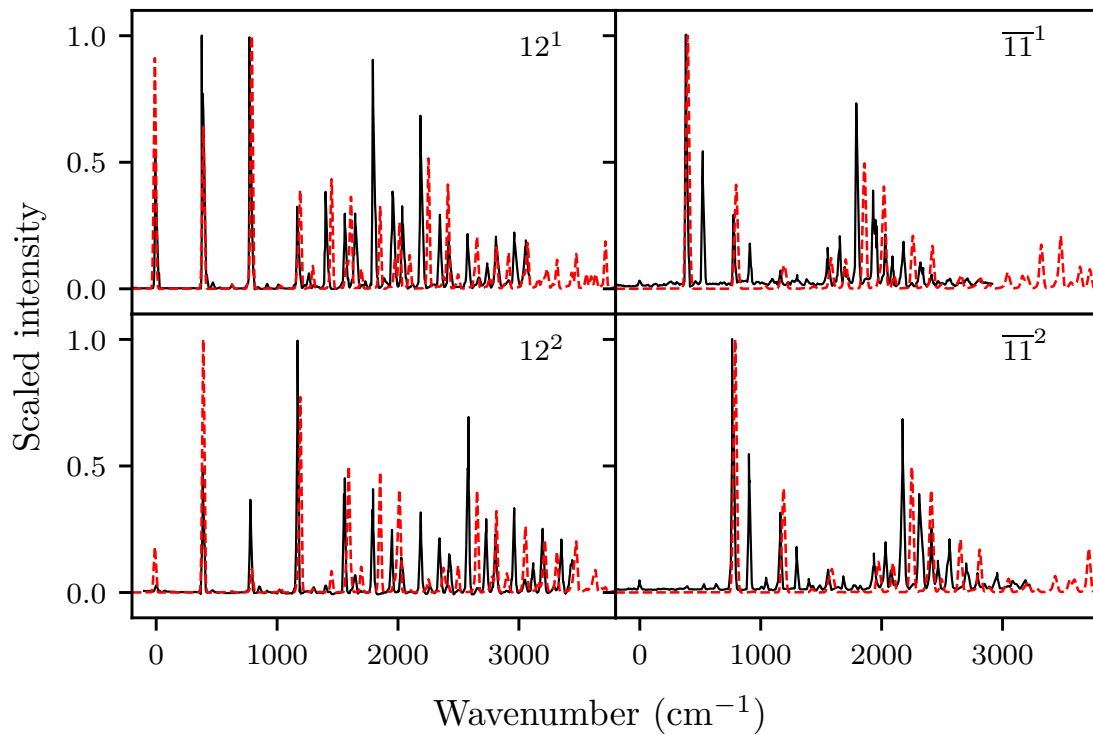


Figure 2: Comparison between the experimental (black solid line) and simulated (red dashed line) SVL fluorescence spectra of anthracene from initial vibrational levels $\overline{11}^j$ and 12^j ($j = 1, 2$), without wavenumber scaling.

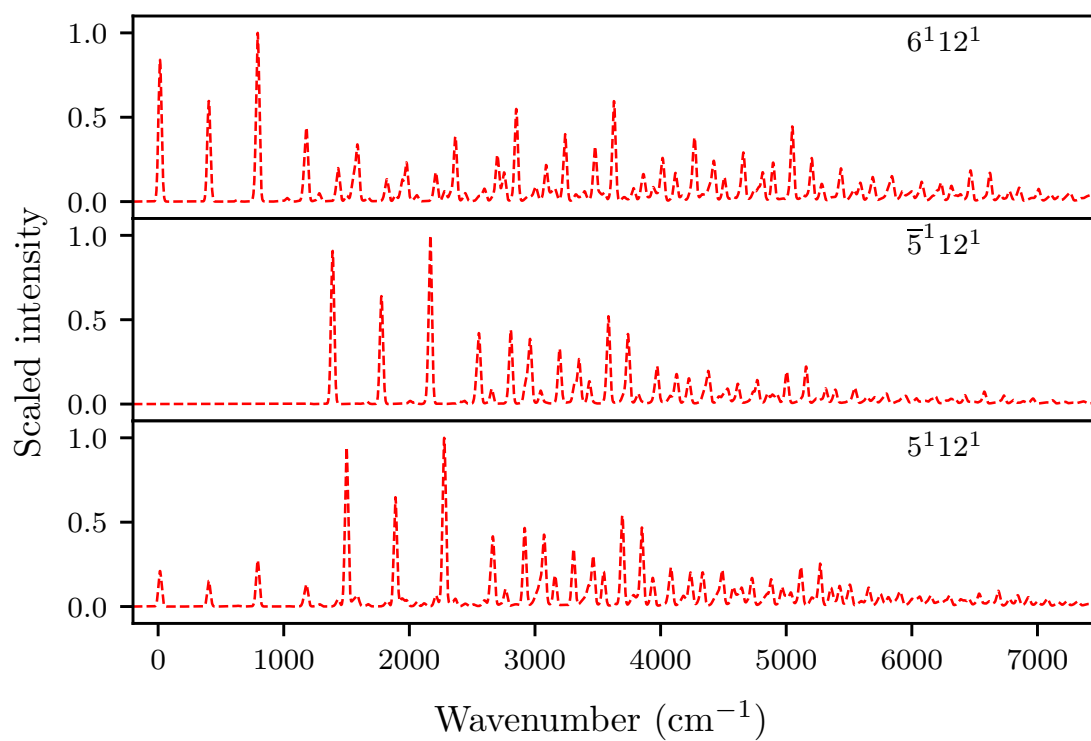


Figure 3: Simulated SVL fluorescence spectra of anthracene from initial vibrational levels $6^1 12^1$, $\bar{5}^1 12^1$, and $5^1 12^1$; a scaling factor of 0.97 is applied to the wavenumbers.

important differences in intensity patterns can be observed due to the excitation in an additional mode. On one hand, we observe that the three peaks in the $< 1000 \text{ cm}^{-1}$ region have weaker intensities in the predicted $5^1 12^1$ spectrum compared to the $6^1 12^1$ one, whereas they completely disappear in the predicted spectrum from the $\bar{5}^1 12^1$ level due to the difference in the symmetry of the modes $\bar{5}$ and 12. On the other hand, the peaks between 1000 cm^{-1} and 2500 cm^{-1} are enhanced in the predicted spectra from levels $\bar{5}^1 12^1$ and $5^1 12^1$ compared to the spectrum from the $6^1 12^1$ level.

Although Hagedorn wavepackets can also be used to simulate spectra from levels with multiple excitations in several modes, we restrict ourselves here to the more experimentally feasible vibronic levels ($6^1 12^1$, $\bar{5}^1 12^1$, and $5^1 12^1$), which were reported respectively at $1380 + 385 \text{ cm}^{-1}$, $1409 + 385 \text{ cm}^{-1}$, and $1420 + 385 \text{ cm}^{-1}$ on the experimental fluorescence excitation spectrum of anthracene, albeit with very weak intensities (2–3% of the signal at origin).⁴ Despite the current lack of experimental data for direct comparison for these levels, the Hagedorn approach can serve as a tool for predicting complex vibronic spectra.

To conclude, we have combined Hagedorn wavepacket dynamics with ab initio DFT evaluation of electronic structure in order to simulate SVL spectroscopy in a realistic molecular system. We were able to compute SVL spectra of anthracene beyond emission from singly excited vibrational levels and in good agreement with experiments. However, it is still limited by the simplifications inherent in the harmonic model^{28,29,72,73} and the quality of the electronic structure data used to construct this model.⁷⁴ In the future, we plan to combine our approach with the local harmonic approximation in order to capture mild anharmonicity effects. An extension of our method could be useful for other experimental techniques involving vibrationally excited states, such as vibrationally promoted electronic resonance (VIPER) experiments,^{75–77} time-resolved photoelectron spectroscopy,⁷⁸ and fluorescence-encoded infrared (FEIR) spectroscopy.⁷⁹

Computational details

As in ref 17, the geometry optimization and frequency calculations were performed using Gaussian 16⁸⁰ at PBE0/def2-TZVP level of theory.^{81,82} The assignment of the vibrational modes follows the supporting information of ref 17. The Gaussian parameters were propagated for a total time of 8×10^5 au (~ 19 ps) with a time step of 8 au. Based on the same Gaussian trajectory, the autocorrelation functions between Hagedorn wavepackets were computed every four steps for each initial vibrational level using the algebraic algorithm described in ref 63. The spectra are broadened by applying a Gaussian damping function with a half-width at half-maximum of 20000 au to the autocorrelation functions.

Acknowledgement

The authors acknowledge the financial support from the EPFL.

References

- (1) Parmenter, C.; Schuyler, M. Fluorescence and nonradiative transitions from single vibronic levels in the excited singlet state of benzene. Transitions non radiatives dans les molécules : 20e réunion de la Société de chimie physique, Paris, 27 au 30 mai 1969. 1970; p 92.
- (2) Woudenberg, T. M.; Kulkarni, S. K.; Kenny, J. E. Internal conversion rates for single vibronic levels of S_2 in azulene. *J. Chem. Phys.* **1988**, *89*, 2789–2796.
- (3) Felker, P. M.; Zewail, A. H. Dynamics of intramolecular vibrational-energy redistribution (IVR). II. Excess energy dependence. *J. Chem. Phys.* **1985**, *82*, 2975–2993.
- (4) Lambert, W. R.; Felker, P. M.; Syage, J. A.; Zewail, A. H. Jet spectroscopy of anthracene and deuterated anthracenes. *J. Chem. Phys.* **1984**, *81*, 2195–2208.

- (5) Lambert, W. R.; Felker, P. M.; Zewail, A. H. Picosecond excitation and selective intramolecular rates in supersonic molecular beams. I. SVL fluorescence spectra and lifetimes of anthracene and deuterated anthracenes. *J. Chem. Phys.* **1984**, *81*, 2209–2216.
- (6) Duca, M. D. The intramolecular vibrational energy redistribution threshold in S₁ deuterated p-difluorobenzene. *Spectrochim. Acta A* **2004**, *60*, 2667–2671.
- (7) Quack, M.; Stockburger, M. Resonance fluorescence of aniline vapour. *J. Mol. Spectrosc.* **1972**, *43*, 87–116.
- (8) Yang, J.; Wagner, M.; Laane, J. Laser-Induced Fluorescence Spectra, Structure, and the Ring-Twisting and Ring-Bending Vibrations of 1,4-Benzodioxan in Its S₀ and S₁ (π, π^*) States. *J. Phys. Chem. A* **2006**, *110*, 9805–9815.
- (9) Hollas, J.; Bin Hussein, M. Z. The C(1)-C(α) torsional potential function of cis- and trans-3-fluorostyrene by supersonic jet spectroscopy. *Chem. Phys. Lett.* **1989**, *154*, 228–233.
- (10) Newby, J. J.; Liu, C.-P.; Müller, C. W.; Zwier, T. S. Jet-cooled vibronic spectroscopy of potential intermediates along the pathway to PAH: phenylcyclopenta-1,3-diene. *Phys. Chem. Chem. Phys.* **2009**, *11*, 8316.
- (11) Barber, V. P.; Newby, J. J. Jet-Cooled Fluorescence Spectroscopy of a Natural Product: Anethole. *J. Phys. Chem. A* **2013**, *117*, 12831–12841.
- (12) Smith, T. C.; Gharaibeh, M.; Clouthier, D. J. Spectroscopic detection of the stannylidene (H₂C=Sn and D₂C=Sn) molecule in the gas phase. *J. Chem. Phys.* **2022**, *157*, 204306.
- (13) Chau, F.-T.; Dyke, J. M.; Lee, E. P.-F.; Wang, D.-C. Franck–Condon analysis of photoelectron and electronic spectra of small molecules. *J. Electron Spectrosc. Relat. Phenom.* **1998**, *97*, 33–47.

- (14) Chau, F.-T.; Dyke, J. M.; Lee, E. P. F.; Mok, D. K. W. Simulation of $A^1B_1 \rightarrow \tilde{X}^1A_1$ CF2 single vibronic level emissions: Including anharmonic and Duschinsky effects. *J. Chem. Phys.* **2001**, *115*, 5816–5822.
- (15) Barbu-Debus, K. L.; Lahmani, F.; Zehnacker-Rentien, A.; Guchhait, N. Laser-induced fluorescence and single vibronic level emission spectroscopy of chiral (R)-1-aminoindan and some of its clusters in a supersonic jet. *Phys. Chem. Chem. Phys.* **2006**, *8*, 1001–1006.
- (16) Lee, E. P. F.; Dyke, J. M.; Mok, D. K. W.; Chow, W.-k.; Chau, F.-T. *Ab initio* calculations on SnCl₂ and Franck-Condon factor simulations of its $\tilde{a} - \tilde{X}$ and $\tilde{B} - \tilde{X}$ absorption and single-vibronic-level emission spectra. *J. Chem. Phys.* **2007**, *127*, 024308.
- (17) Tapavicza, E. Generating Function Approach to Single Vibronic Level Fluorescence Spectra. *J. Phys. Chem. Lett.* **2019**, *10*, 6003–6009.
- (18) Tarroni, R.; Clouthier, D. J. *Ab initio* spectroscopy of the aluminum methylene (AlCH₂) free radical. *J. Chem. Phys.* **2020**, *153*, 014301.
- (19) Sunahori, F. X.; Smith, T. C.; Clouthier, D. J. Spectroscopic identification and characterization of the aluminum methylene (AlCH₂) free radical. *J. Chem. Phys.* **2022**, *157*, 044301.
- (20) Grimminger, R.; Clouthier, D. J.; Tarroni, R.; Wang, Z.; Sears, T. J. An experimental and theoretical study of the electronic spectrum of HPS, a second row HNO analog. *J. Chem. Phys.* **2013**, *139*, 174306.
- (21) Carrington, T. In *Handbook of High-resolution Spectroscopy*; Quack, M., Merkt, F., Eds.; Wiley, 2011.

- (22) Borrelli, R.; Capobianco, A.; Peluso, A. Franck–Condon factors — Computational approaches and recent developments. *Can. J. Chem.* **2013**, *91*, 495–504.
- (23) Meier, P.; Rauhut, G. Comparison of methods for calculating Franck–Condon factors beyond the harmonic approximation : how important are Duschinsky rotations? *Mol. Phys.* **2015**, *113*, 3859–3873.
- (24) Conte, R.; Aieta, C.; Botti, G.; Cazzaniga, M.; Gandolfi, M.; Lanzi, C.; Mandelli, G.; Moscato, D.; Ceotto, M. Anharmonicity and quantum nuclear effects in theoretical vibrational spectroscopy: a molecular tale of two cities. *Theor. Chem. Acc.* **2023**, *142*.
- (25) Baiardi, A.; Bloino, J.; Barone, V. General Time Dependent Approach to Vibronic Spectroscopy Including Franck-Condon, Herzberg-Teller, and Duschinsky Effects. *J. Chem. Theory Comput.* **2013**, *9*, 4097–4115.
- (26) Wehrle, M.; Šulc, M.; Vaníček, J. On-the-fly Ab Initio Semiclassical Dynamics: Identifying Degrees of Freedom Essential for Emission Spectra of Oligothiophenes. *J. Chem. Phys.* **2014**, *140*, 244114.
- (27) Wehrle, M.; Oberli, S.; Vaníček, J. On-the-fly ab initio semiclassical dynamics of floppy molecules: Absorption and photoelectron spectra of ammonia. *J. Phys. Chem. A* **2015**, *119*, 5685.
- (28) Bonfanti, M.; Petersen, J.; Eisenbrandt, P.; Burghardt, I.; Pollak, E. Computation of the S1 S0 vibronic absorption spectrum of formaldehyde by variational Gaussian wavepacket and semiclassical IVR methods. *J. Chem. Theory Comput.* **2018**, *14*, 5310–4323.
- (29) Koch, W.; Bonfanti, M.; Eisenbrandt, P.; Nandi, A.; Fu, B.; Bowman, J.; Tannor, D.; Burghardt, I. Two-layer Gaussian-based MCTDH study of the S1 ← S vibronic absorption spectrum of formaldehyde using multiplicative neural network potentials. *J. Chem. Phys.* **2019**, *151*, 064121.

- (30) Begušić, T.; Tapavicza, E.; Vaníček, J. Applicability of the Thawed Gaussian Wavepacket Dynamics to the Calculation of Vibronic Spectra of Molecules with Double-Well Potential Energy Surfaces. *J. Chem. Theory Comput.* **2022**, *18*, 3065–3074.
- (31) Huh, J.; Berger, R. Coherent state-based generating function approach for Franck–Condon transitions and beyond. *Journal of Physics: Conference Series* **2012**, *380*, 012019.
- (32) Borrelli, R.; Capobianco, A.; Peluso, A. Generating function approach to the calculation of spectral band shapes of free-base chlorin including Duschinsky and Herzberg-Teller effects. *J. Phys. Chem. A* **2012**, *116*, 9934–9940.
- (33) Patoz, A.; Begušić, T.; Vaníček, J. On-the-Fly Ab Initio Semiclassical Evaluation of Absorption Spectra of Polyatomic Molecules beyond the Condon Approximation. *J. Phys. Chem. Lett.* **2018**, *9*, 2367–2372.
- (34) Begušić, T.; Patoz, A.; Šulc, M.; Vaníček, J. On-the-fly ab initio three thawed Gaussians approximation: a semiclassical approach to Herzberg-Teller spectra. *Chem. Phys.* **2018**, *515*, 152–163.
- (35) Prlj, A.; Begušić, T.; Zhang, Z. T.; Fish, G. C.; Wehrle, M.; Zimmermann, T.; Choi, S.; Roulet, J.; Moser, J.-E.; Vaníček, J. Semiclassical Approach to Photophysics Beyond Kasha’s Rule and Vibronic Spectroscopy Beyond the Condon Approximation. The Case of Azulene. *J. Chem. Theory Comput.* **2020**, *16*, 2617–2626.
- (36) Kundu, S.; Roy, P. P.; Fleming, G. R.; Makri, N. Franck-Condon and Herzberg-Teller signatures in molecular absorption and emission spectra. *J. Phys. Chem. B* **2022**, *126*, 2899–2911.
- (37) Borrelli, R.; Gelin, M. F. Quantum electron-vibrational dynamics at finite temperature: Thermo field dynamics approach. *J. Chem. Phys.* **2016**, *145*, 224101.

- (38) Begušić, T.; Vaníček, J. On-the-fly ab initio semiclassical evaluation of vibronic spectra at finite temperature. *J. Chem. Phys.* **2020**, *153*, 024105.
- (39) Begušić, T.; Vaníček, J. Efficient semiclassical dynamics for vibronic spectroscopy beyond harmonic, Condon, and zero-temperature approximations. *Chimia* **2021**, *75*, 261.
- (40) Gelin, M. F.; Borrelli, R. Thermo-Field Dynamics Approach to Photo-induced Electronic Transitions Driven by Incoherent Thermal Radiation. *J. Chem. Theory Comput.* **2023**, *19*, 6402–6413.
- (41) Schubert, A.; Engel, V. Two-dimensional vibronic spectroscopy of coherent wave-packet motion. *J. Chem. Phys.* **2011**, *134*, 104304.
- (42) Begušić, T.; Vaníček, J. On-the-fly ab initio semiclassical evaluation of third-order response functions for two-dimensional electronic spectroscopy. *J. Chem. Phys.* **2020**, *153*, 184110.
- (43) Begušić, T.; Vaníček, J. Finite-temperature, anharmonicity, and Duschinsky effects on the two-dimensional electronic spectra from ab initio thermo-field Gaussian wavepacket dynamics. *J. Phys. Chem. Lett.* **2021**, *12*, 2997–3005.
- (44) Gelin, M. F.; Chen, L.; Domcke, W. Equation-of-Motion Methods for the Calculation of Femtosecond Time-Resolved 4-Wave-Mixing and N-Wave-Mixing Signals. *Chem. Rev.* **2022**, *122*, 17339–17396.
- (45) Zhang, Z. T.; Vaníček, J. J. L. Single vibronic level fluorescence spectra from Hagedorn wavepacket dynamics. 2024; arXiv: 2403.00577 [physics.chem-ph].
- (46) Hagedorn, G. A. Raising and Lowering Operators for Semiclassical Wave Packets. *Ann. Phys. (NY)* **1998**, *269*, 77–104.
- (47) Faou, E.; Gradinaru, V.; Lubich, C. Computing semiclassical quantum dynamics with Hagedorn wavepackets. *SIAM J. Sci. Comp.* **2009**, *31*, 3027–3041.

- (48) Lasser, C.; Lubich, C. Computing quantum dynamics in the semiclassical regime. *Acta Numerica* **2020**, *29*, 229–401.
- (49) Lasser, C.; Troppmann, S. Hagedorn Wavepackets in Time-Frequency and Phase Space. *J. Fourier Anal. Appl.* **2014**, *20*, 679–714.
- (50) Ohsawa, T. The Hagedorn–Hermite Correspondence. *J. Fourier Anal. Appl.* **2019**, *25*, 1513–1552.
- (51) Kargol, A. Semiclassical scattering by the Coulomb potential. *Annales de l’I.H.P. Physique théorique* **1999**, *71*, 339–357.
- (52) Hagedorn, G.; Joye, A. Exponentially Accurate Semiclassical Dynamics: Propagation, Localization, Ehrenfest Times, Scattering, and More General States. *Ann. Henri Poincaré* **2000**, *1*, 837–883.
- (53) Gradinaru, V.; Hagedorn, G. A.; Joye, A. Exponentially accurate semiclassical tunneling wavefunctions in one dimension. *J. Phys. Math. Theor.* **2010**, *43*, 474026.
- (54) Gradinaru, V.; Hagedorn, G. A.; Joye, A. Tunneling dynamics and spawning with adaptive semiclassical wave packets. *J. Chem. Phys.* **2010**, *132*, 184108.
- (55) Lubich, C. *From Quantum to Classical Molecular Dynamics: Reduced Models and Numerical Analysis*, 12th ed.; European Mathematical Society: Zürich, 2008.
- (56) Dietert, H.; Keller, J.; Troppmann, S. An invariant class of wave packets for the Wigner transform. *J. Math. Anal. Appl.* **2017**, *450*, 1317–1332.
- (57) Ohsawa, T. Symplectic semiclassical wave packet dynamics II: non-Gaussian states. *Nonlinearity* **2018**, *31*, 1807–1832.
- (58) Bourquin, R.; Gradinaru, V.; Hagedorn, G. A. Non-adiabatic transitions near avoided crossings: theory and numerics. *J. Math. Chem.* **2012**, *50*, 602–619.

- (59) Kieri, E.; Holmgren, S.; Karlsson, H. O. An adaptive pseudospectral method for wave packet dynamics. *J. Chem. Phys.* **2012**, *137*, 044111.
- (60) Zhou, Z. Numerical approximation of the Schrödinger equation with the electromagnetic field by the Hagedorn wave packets. *J. Comput. Phys.* **2014**, *272*, 386–407.
- (61) Gradinaru, V.; Rietmann, O. Hagedorn wavepackets and Schrödinger equation with time-dependent, homogeneous magnetic field. *J. Comput. Phys.* **2021**, *445*, 110581.
- (62) Gradinaru, V.; Rietmann, O. Spawning semiclassical wavepackets. *J. Comput. Phys.* **2024**, *509*, 113029.
- (63) Vaníček, J. J. L.; Zhang, Z. T. On Hagedorn wavepackets associated with different Gaussians. 2024; arXiv: 2405.07880 [quant-ph].
- (64) Heller, E. J. The semiclassical way to molecular spectroscopy. *Acc. Chem. Res.* **1981**, *14*, 368–375.
- (65) Vaníček, J. J. L. Family of Gaussian wavepacket dynamics methods from the perspective of a nonlinear Schrödinger equation. *J. Chem. Phys.* **2023**, *159*, 014114.
- (66) Hagedorn, G. A. Semiclassical quantum mechanics. I. The $\hbar \rightarrow 0$ limit for coherent states. *Commun. Math. Phys.* **1980**, *71*, 77–93.
- (67) Begušić, T.; Cordova, M.; Vaníček, J. Single-Hessian thawed Gaussian approximation. *J. Chem. Phys.* **2019**, *150*, 154117.
- (68) Klētnieks, E.; Alonso, Y. C.; Vaníček, J. J. L. Isotope effects on the electronic spectra of ammonia from ab initio semiclassical dynamics. *J. Phys. Chem. A* **2023**, *127*, 8117–8125.
- (69) Wenzel, M.; Mitric, R. Internal conversion rates from the extended thawed Gaussian approximation: theory and validation. *J. Chem. Phys.* **2023**, *158*, 034105.

- (70) Wenzel, M.; Mitric, R. Prediction of fluorescence quantum yields using the extended thawed Gaussian approximation. *J. Chem. Phys.* **2023**, *159*, 234113.
- (71) Computational Chemistry Comparison and Benchmark Database, NIST Standard Reference Database Number 101. <http://cccbdb.nist.gov/>, 2022; Release 22, May 2022. Accessed: 2024-02-04.
- (72) Conte, R.; Botti, G.; Ceotto, M. Sensitivity of semiclassical vibrational spectroscopy to potential energy surface accuracy: A test on formaldehyde. *Vib. Spectrosc.* **2020**, *106*, 103015.
- (73) Barbiero, D.; Bertaina, G.; Ceotto, M.; Conte, R. Anharmonic Assignment of the Water Octamer Spectrum in the OH Stretch Region. *J. Phys. Chem. A* **2023**, *127*, 6213–6221.
- (74) Tatchen, J.; Pollak, E. Ab initio spectroscopy and photoinduced cooling of the trans-stilbene molecule. *J. Chem. Phys.* **2008**, *128*, 164303.
- (75) van Wilderen, L. J. G. W.; Messmer, A. T.; Bredenbeck, J. Mixed IR/Vis Two-Dimensional Spectroscopy: Chemical Exchange beyond the Vibrational Lifetime and Sub-ensemble Selective Photochemistry. *Angew. Chem. Int. Ed.* **2014**, *53*, 2667–2672.
- (76) Von Cosel, J.; Cerezo, J.; Kern-Michler, D.; Neumann, C.; Van Wilderen, L. J. G. W.; Bredenbeck, J.; Santoro, F.; Burghardt, I. Vibrationally resolved electronic spectra including vibrational pre-excitation: Theory and application to VIPER spectroscopy. *J. Chem. Phys.* **2017**, *147*, 164116.
- (77) Horz, M.; Masood, H. M. A.; Brunst, H.; Cerezo, J.; Picconi, D.; Vormann, H.; Niraghatam, M. S.; Van Wilderen, L. J. G. W.; Bredenbeck, J.; Santoro, F. et al. Vibrationally resolved two-photon electronic spectra including vibrational pre-excitation: Theory and application to VIPER spectroscopy with two-photon excitation. *J. Chem. Phys.* **2023**, *158*, 064201.

- (78) Yu, H.; Evans, N. L.; Chatterley, A. S.; Roberts, G. M.; Stavros, V. G.; Ullrich, S. Tunneling Dynamics of the NH₃ (\tilde{A}) State Observed by Time-Resolved Photoelectron and H Atom Kinetic Energy Spectroscopies. *J. Phys. Chem. A* **2014**, *118*, 9438–9444.
- (79) Whaley-Mayda, L.; Guha, A.; Penwell, S. B.; Tokmakoff, A. Fluorescence-Encoded Infrared Vibrational Spectroscopy with Single-Molecule Sensitivity. *J. Am. Chem. Soc.* **2021**, *143*, 3060–3064.
- (80) Frisch, M. J.; Trucks, G. W.; Schlegel, H. B.; Scuseria, G. E.; Robb, M. A.; Cheeseman, J. R.; Scalmani, G.; Barone, V.; Petersson, G. A.; Nakatsuji, H. et al. Gaussian 16 Revision C.01. 2016; Gaussian Inc. Wallingford CT.
- (81) Adamo, C.; Barone, V. Toward reliable density functional methods without adjustable parameters: The PBE0 model. *J. Chem. Phys.* **1999**, *110*, 6158–6170.
- (82) Weigend, F.; Ahlrichs, R. Balanced basis sets of split valence, triple zeta valence and quadruple zeta valence quality for H to Rn: Design and assessment of accuracy. *Phys. Chem. Chem. Phys.* **2005**, *7*, 3297.